

High-Throughput Platform for Fluorescence Image-Based Neurite Outgrowth Analysis

Automated solution for quantitative neurite outgrowth analysis of labeled iPSC-derived and primary neuron culture models

Authors

Rebecca Mongeon, PhD
Sarah Guadiana, PhD
Joe Clayton, PhD
Agilent Technologies, Inc.

Abstract

The evaluation of neurite outgrowth using high-throughput image-based analysis provides an essential tool for neurobiologists to advance basic, translational, and clinical research in neuroscience. In this application note, we introduce the Agilent BioTek Gen5 neurite outgrowth module for flexible, automated, multichannel analysis of neurite outgrowth. The module is compatible across Agilent BioTek imaging instruments to provide a single platform solution for neurite outgrowth assays. Neurite outgrowth analysis capabilities are demonstrated through proof-of-principle outgrowth evaluations for both iPSC-derived and primary neuron culture models. Automated image collection and analysis was performed in a high-density microplate format that enabled dose-response analysis of neuron cultures with multiple neurite outgrowth characteristics. Fluorescent immunocytochemistry-based evaluations yielded sensitive and specific detection of both stimulatory and inhibitory effects on outgrowth parameters in both neuron culture models.

Introduction

Neurons extend cellular outgrowths in a coordinated set of developmental processes that serve to both establish and maintain the cellular connections essential to the nervous system's communications network. These early outgrowth processes, termed neurites, are developing dendrite and axon compartments that will be responsible for incoming and outgoing neurotransmission, respectively. In vitro neurite outgrowth models have provided an essential platform for determining the molecular and cellular mechanisms that underlie both normal and aberrant neuronal development.¹ Furthermore, neurite outgrowth plays a role in key neurological health research areas focused on leveraging emerging stem cell-derived models for developmental neurotoxicity testing, neuroregeneration, and neurodegeneration.²⁻⁴

Models used for in vitro neurite outgrowth evaluations have historically been acquired from primary murine tissues, and immortalized neuronal-like cell lines typically derived from malignant tissue sources. Although both model types have been essential for foundational research, these models present limitations for scalability, relevance, and predictive power in neurological research.⁵ Comparatively, induced pluripotent stem cell-derived (iPSC-derived) neuronal models have a compelling profile for both translational and clinical research owing to their established relevance and scalability. Furthermore, iPSC-derived cell amenability to genome editing techniques paired with the ability to apply human-derived genetic backgrounds provide powerful handles for neuronal disease phenotyping and personalized medicine.⁵

Neurite outgrowth is evaluated across neuronal culture models using many imaging techniques, including label-free methods, live-cell stains, membrane dyes, and antibody-based immunofluorescence. Of these, antibody-based staining is often relied upon for neuron detection, as it provides a level of specificity that cannot be readily matched by alternative methods. Antibody-based staining is clearly required for neurite outgrowth analysis in complex culture models, such as coculture or triculture model systems. However, specificity can also be important for outgrowth in models where neuronal differentiation is only occurring in a subpopulation of cultured cells through addition or exclusion of media factors.^{6,7} Primary cortical cultures also present mixed cell populations that benefit from antibody-based analysis for specificity, although tissue age and media components can be leveraged to limit the presence and expansion of nonneuronal cell populations.⁸ iPSC-derived neuronal cultures, such as the iCell GlutaNeurons used in this study, can provide a high degree of pure neuronal populations, but antibody-based evaluations are often still relied upon to establish neuronal marker expression and outgrowth.⁹

The Agilent BioTek Gen5 neurite outgrowth module, used with an Agilent BioTek cell imaging multimode reader, provides a flexible and powerful system to support neurite outgrowth research. This study demonstrates neuron culture outgrowth analysis using advanced immunohistochemistry techniques that focus on multiplexed fluorescent analysis of two commonly used culture models for neurite outgrowth. We detail how automation of sample preparation steps, image collection, and image analysis can facilitate the sensitive, high-throughput evaluation of neurite outgrowth while minimizing user intervention and effort. Positive and negative chemical modulators of neurite outgrowth are evaluated to demonstrate the sensitivity and performance of the platform to detect changes across multiple parameters relevant for neurite outgrowth assays.

Experimental

Materials

Chemicals

All chemicals were purchased from Sigma unless otherwise noted, including outgrowth effectors blebbistatin (p/n B0560), 6BIO (p/n B1686), and triptolide (p/n T3652). Staurosporine was purchased from Tocris Bioscience (p/n 1285).

Cell culture

iCell GlutaNeurons (FUJIFILM Cellular Dynamics, Inc., p/n R1061) cryopreserved iPSC-derived neurons were cultured in BrainPhys Neuronal Medium (StemCell Technologies, p/n 05790) supplemented with iCell Neural Supplement B (iCell kit component), iCell Nervous System Supplement (iCell kit component), N-2 Supplement (Gibco, p/n 17502048), and laminin (Sigma, L2020). Primary mouse cortical neurons (Gibco, p/n A15586) were cultured in NeuroCult Neuronal Plating Medium (StemCell Technologies, p/n 05713) and supplemented with NeuroCult SM1 neuronal supplement (StemCell Technologies, p/n 05711), GlutaMAX supplement (Gibco, 35050061), L-glutamate (Sigma, p/n 1251), and laminin (Sigma, p/n L2020). iCell GlutaNeuron and primary mouse cultures were plated on Greiner glass bottom 96-well microplates (Greiner, p/n 655892) for outgrowth assays. Microplates for iCell GlutaNeuron cultures were first coated with poly-L-ornithine solution (PLO: Sigma, A-004-M), followed by complete media supplemented with laminin. Microplates for mouse cortical neurons were coated with poly-D-lysine (Gibco, p/n A3890401).

Immunohistochemistry

Anti- β -tubulin III antibody (β -tubulin) was purchased from Sigma (p/n T8578) and anti-MAP2 antibody (MAP2) was purchased from Invitrogen (p/n PA1-10005). Goat-anti-mouse Alexa 633 secondary antibody was purchased from Thermo Fisher Scientific (p/n A21052) and goat-anti-chicken Alexa 488 secondary antibody was purchased from Invitrogen (p/n A11039). Bovine serum albumin (BSA) was purchased from Sigma (p/n A3294).

Instrumentation

The Agilent BioTek Cytation 5 cell imaging multimode reader with wide field of view camera was used for all image acquisition and was outfitted with a 20x phase contrast objective (p/n 1320517) and the following filter cubes: DAPI (p/n 1225100), GFP (p/n 1225101), CY5 (p/n 1225105), and LAF (p/n 1225010). The Agilent BioTek MultiFlo FX multimode dispenser with the Agilent BioTek Automated Media Exchange (AMX) module was used for plate washes between immunohistochemistry steps. The Gen5 neurite outgrowth module was used for all image analysis and data plotting.

Methods

Cell culture

Culture procedures followed manufacturer recommendations for iCell GlutaNeurons and cryopreserved mouse cortical neurons. Microplates were prepared for culture the day before plating. Plates were first coated overnight at room temperature with poly-L-ornithine (iCell GlutaNeurons) or poly-D-lysine (mouse cortical neurons). Coated plates were rinsed five times with sterile phosphate-buffered saline (PBS) and incubated in a humidified tissue culture incubator (at 37 °C and 5% CO₂) for at least one hour before plating cells with complete media (mouse cortical neurons), or complete media plus laminin (iCell GlutaNeurons).

iCell GlutaNeuron and cryopreserved mouse cortical neurons were thawed and plated following manufacturer protocol recommendations. Live cell estimations were performed with trypan blue exclusion method. Cells were plated at a density of approximately 10,000 live cells per well. To promote even cell dispersal across the well, plates were allowed to rest at room temperature for approximately 30 minutes to permit cell adhesion before transferring to a tissue culture incubator. To minimize evaporative effects across the plate, regions between wells were partially filled with sterile water. For mouse cortical cultures, a 50% media exchange was performed approximately two hours after initial plating.

After 24 hours of initial outgrowth, a dilution series of outgrowth effectors were applied to both iCell GlutaNeuron and mouse primary cortical culture in a 50% media exchange. For iCell GlutaNeurons only, an additional 50% media exchange was performed 48 hours later (72 hours following plating) with maintenance of final drug concentrations.

Immunohistochemistry processing

After five days in vitro (120 hours), cultures were fixed with 4% paraformaldehyde for 15 minutes at room temperature. Following fixation, 96-well microplates were washed with PBS with 0.05% Tween-20 (PBST) using the MultiFlo FX with the AMX module for five cycles (150 μ L per cycle, 30 μ L/second).

Cultures were permeabilized and blocked for one hour at room temperature with a PBS solution containing 0.1% TritonX-100 and 3% BSA. Permeabilized cultures were incubated overnight at 4 °C with primary antibodies diluted at 1:5,000 in a PBST solution with 3% BSA. Following overnight incubation in primary antibody, plates were washed five times with the MultiFlo FX with AMX module. Secondary antibodies were applied at a 1:500 dilution in PBST containing 1% BSA and 1 μ M DAPI nuclear counterstain and incubated for two hours at room temperature. Following secondary antibody incubation, plates were washed five times with a MultiFlo FX with AMX module with PBST + 0.05% sodium azide.

Image capture and processing

Multichannel fluorescence images were captured at 20x magnification in widefield mode in a 3 x 3 image montage in the center of each well across the 96-well plate. Focus was achieved using the laser autofocus method. Image tiles were stitched to generate a single large image for neurite outgrowth analysis. Stitched images were background subtracted (100 μ m rolling ball) before analysis for optimal visualization of neuronal processes.

Image analysis

Default settings of the Gen5 neurite outgrowth module provided a starting point for soma and neurite detection and were further optimized as shown in Table 1. For best results with immunolabeled cultures, it is recommended that both immunostaining and nuclear staining signals are used for soma detection. Optimal values for the parameters indicated in Table 1 will vary based on experimental conditions, and users are expected to evaluate and adjust these parameters as needed.

Table 1. Neurite outgrowth analysis detection settings.

Neurite Outgrowth Analysis Settings		
Soma Detection	iPSC-derived β -tubulin (CY5) and MAP2 (GFP) channels	Mouse cortical culture β -tubulin (CY5) channel
Threshold Slider Level	20	30
Minimum/Maximum Size	10/100	10/100
Soma Closing Size	0	0
Optimize Soma Using Nuclear Signal	Checked	Checked
Rolling Ball Diameter	20	30
Nucleus Detection (DAPI Channel)		
Threshold Slider Level	40	60
Minimum/Maximum Size	8/50	9.5/50
Minimum Nucleus/Soma Overlap	20	20
Maximum Nucleus/Soma Distance	5	8
Neurites		
Threshold Slider Level	Neutral	Neutral
Neurite Mask Closing Size	0	0
Rolling Ball Diameter	10	15
Only Keep Neurites Connected to a Soma	Checked	Checked
Discard Short Neurites	10	10
Discard Short Ending Branches	5	8

Data analysis and fitting

Gen5 microplate reader and imager software was used for all data plotting and fitting. Dose–response relationships were fit with four-parameter fits and Z-scores were calculated in Gen5 using the difference between the treatment mean and control mean expressed in multiples of the standard deviation of control. In the Gen5 software syntax, the following formula was applied in a transformation step to calculate the Z-score for each outgrowth parameter: $(X - \text{MEAN}(\text{CTL1})) / \text{SD}(\text{CTL1})$

Results and discussion

Neurite outgrowth assay overview

Neurite outgrowth assays are relied upon across neuroscience model systems to evaluate the characteristics of neuron growth and extension of processes in both compromised and healthy states, as well as in response to drug treatment. In this study, two cell models frequently evaluated through neurite outgrowth assays, mouse cortical culture, and iPSC-derived neurons, were explored in a proof-of-concept demonstration of the Gen5 neurite outgrowth module.

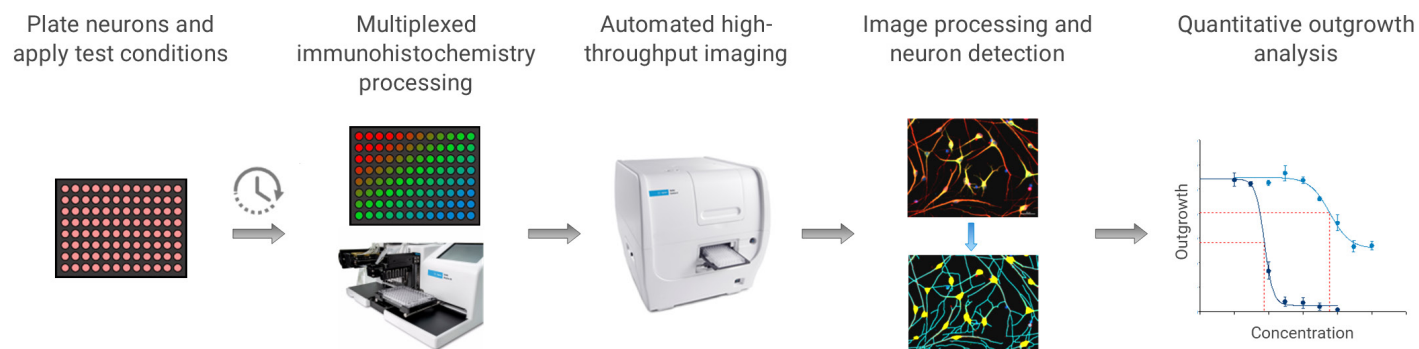


Figure 1. Generalized workflow for immunofluorescence-based automated neurite outgrowth assays.

A general neurite outgrowth assay schematic for immunohistochemistry is shown in Figure 1. Cultures were plated on high-density microplates and processed for evaluation after five days of outgrowth. Multiplexed immunohistochemistry was conducted using two markers for neurite outgrowth and a nuclear counterstain. The MultiFlo FX multimode dispenser with AMX was used for gentle plate washes between immunohistochemistry steps to both maximize efficiency and minimize potential damage from manual pipetting. Multichannel fluorescent images were automatically captured on the Cytation 5 cell imaging multimode reader across the plate and analyzed with Gen5 neurite outgrowth module. Multiple types of analysis, including dose–response analysis shown in Figure 1, can be performed in Gen5 software to evaluate treatment effects on outgrowth.

Image collection and processing for neurite outgrowth analysis

Image-based neurite outgrowth measurements used multichannel fluorescent immunocytochemistry to evaluate two neurite outgrowth markers and nuclear counterstain as outlined in Figure 2. A 20x objective was used for all image acquisition and images were tiled to sample a large region for analysis (Figure 2A, left panel). Montages were stitched together automatically to evaluate a representative central FOV in the well (Figure 2A, center panel). Images were next background subtracted to aid in visualization of neuronal processes (Figure 2A, right panel). Background subtraction is an optional step that is not required for analysis but can help optimize visualization of neurites for display of the analysis results. Background subtraction yielded relatively minor improvements with these cultures as observed by comparing Figure 2A center and right panels. Individual fluorescent channels are shown in Figure 2B with a composite overlay. In maturing neurons, MAP2 antibody labeling is primarily localized to dendrites, whereas the β -tubulin antibody labels both axonal and dendritic compartments. This compartmentation can be appreciated in the overlay image where MAP2-positive neurites are also β -tubulin positive, but many more processes, potentially the developing axonal compartments, are labeled only by the β -tubulin antibody.

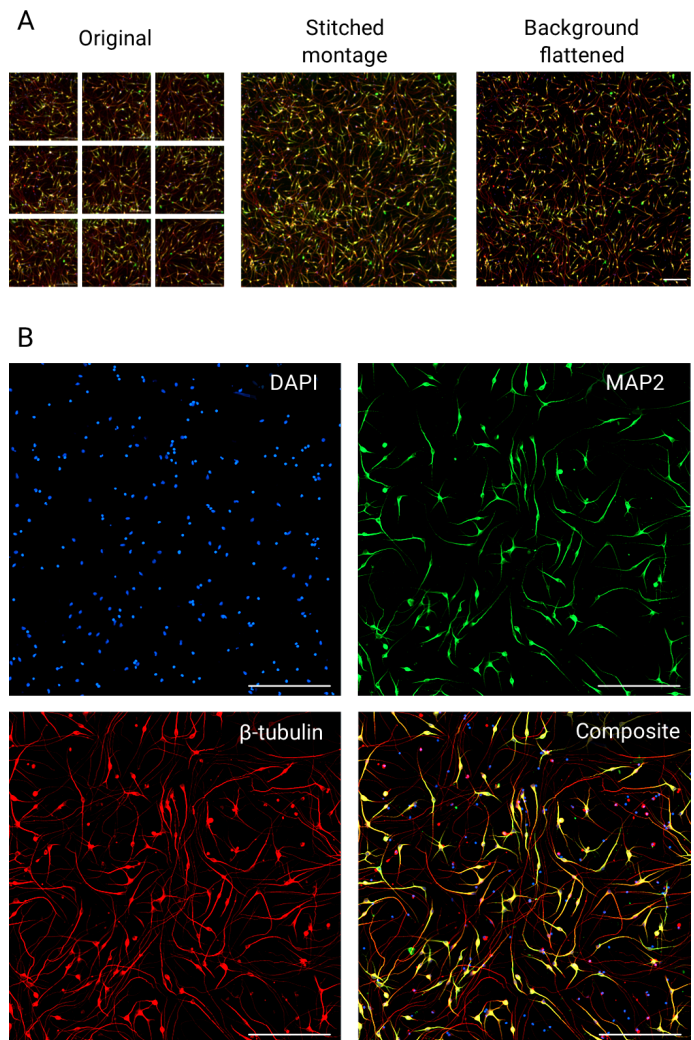


Figure 2. Automated image capture, processing steps, and example immunocytochemistry results. (A) 20x magnification images are automatically captured in multichannel acquisition on an Agilent BioTek Cytation 5 cell imaging multimode reader in widefield mode. A 3 x 3 image panel is captured for each well (left panel) and images are automatically stitched to generate a large image montage for analysis (center panel). Optional background subtraction can be automatically applied to improve the visualization of neurite processes (right panel). (B) Example multichannel images of cryopreserved iPSC-derived neuron cultures after five days in culture stained with DAPI nuclear marker (top left), MAP2 antibody (top right), β -tubulin antibody (bottom left) and composite overlay image for all channels (bottom right). Scale bars correspond to 200 μ m.

Multichannel fluorescent image-based neurite outgrowth analysis

Multichannel montaged images were processed for neurite outgrowth analysis for both β -tubulin and MAP2 staining stepwise as indicated in Figure 3. Gen5 software neurite outgrowth module supports analysis on a single fluorescent channel (e.g., neuron staining) or can combine a second fluorescent channel (e.g., DAPI staining) to optimize detection. For neurite analysis with immunolabeled cultures, it is recommended that both nuclear staining and immunolabeling are used together for optimal results (Figure 3A).

The combination of nuclear staining with immunolabeling helps optimize soma detection in several aspects. First, many neuronal antibodies, including both β -tubulin and MAP2 antibodies, strongly identify the perinuclear somatic region, but are weak or absent in the nucleus itself. Nuclear labels effectively fill these immunolabeling voids for improved soma segmentation. Second, the Gen5 neurite outgrowth module uses nuclear signals to help separate clusters of neuronal somas and can therefore provide more accurate soma counts.

Third, Gen5 neurite outgrowth module includes built-in options designed to leverage nuclear signals to limit the detection of nonneuronal nuclei through a minimum percent overlap criteria between the nuclear and somatic staining signals. Finally, nuclear staining provides a means of setting a distance limit for how far the soma signal can extend from the nucleus, termed the nucleus/soma distance in Gen5 neurite outgrowth module. This feature assists in defining the boundary of where the soma ends and the neurite begins and can be adjusted according to user requirements. Soma identification, depicted in Figure 3B, was identified with this purpose-built combination of Gen5 neurite outgrowth module features to accurately identify viable neuronal somas for analysis.

Following soma detection optimization, neurite detection was next optimized as shown in Figure 3C. Gen5 neurite outgrowth module neurite filtering features provide the ability to include or disregard detected neurites according to several criteria. First, users can opt to include only neurites that are connected to soma on the image for analysis. Electing this filtering option will discard fragmented neurites and neurites that originate from soma that are not within the image. The neurite skeletons displayed in Figure 3C were filtered to only include neurites connected to somas. However, it should be noted that the images shown in Figure 3C are only a portion of the entire field that was analyzed, and it is expected that some neurites displayed connect to soma that are not visible within the displayed region.

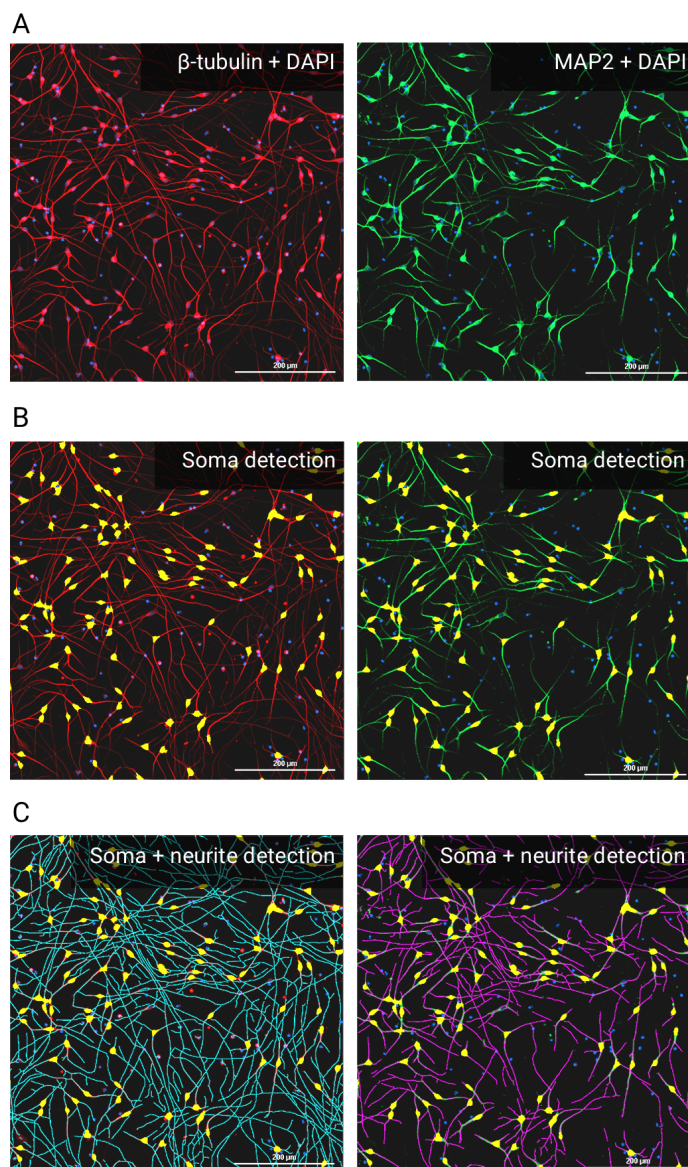


Figure 3. Immunocytochemistry-based neurite outgrowth detection optimization for soma and neurites. (A) Example images of fluorescent antibody staining for β -tubulin and MAP2 antibodies with DAPI nuclear counterstaining, as indicated. The displayed image is a subregion of the entire montage for display purposes. (B) The same image from panel A overlaid with soma detection results (yellow solid mask overlay) for β -tubulin (left panel) and MAP2 antibody (right panel) staining channels. Detected soma were filtered based on multiple criteria including nuclear size, and minimal overlap between the soma stain and nuclear stain. (C) Neurite analysis results for β -tubulin (left panel) and MAP2 antibody (right panel) staining shown with both soma mask overlay (solid yellow fill) and neurite skeleton overlay (left panel: cyan, right panel: magenta). Neurite skeleton overlay displays were increased to three-pixel width for improved visualization. Scale bars correspond to 200 μ m.

Additional filtering options permit users to set minimal requirements to include neurites for analysis, such as minimal acceptable lengths for fragmented neurites, neurites extending directly from a soma, and terminal neurite branches.

Neuron outgrowth response to inhibitors and enhancers of neurite outgrowth

As a proof-of-principle demonstration, outgrowth of cryopreserved iPSC-derived neuron and primary mouse cortical neuron cultures were evaluated in response to treatment with four drugs previously reported as potential enhancers or inhibitors of neurite outgrowth.⁹ Cells were plated at a density of 10,000 live cells (determined via post-thaw trypan blue cell counting) per well in a 96-well plate format for outgrowth evaluation. For iCell GlutaNeurons, a live cell percentage of approximately 65% was observed at thaw and total live-cell yields were consistent with the manufacturer estimates. For cryopreserved mouse ECNs, a live cell percentage of approximately 50% was observed at thaw, also in line with the manufacturer's estimates.

At 24 hours post-thaw (culture day 1), 50% of the neuron culture media was removed and replaced with a dilution series of each of the four drugs at the final concentrations indicated in Figure 4A. After 48 hours of drug exposure (culture day 3), an additional 50% media exchange was performed for iCell GlutaNeurons (while maintaining final drug concentrations), in alignment with the manufacturer's recommendations for media refreshment schedule. Media exchanges between culture days 1 and 5 were not performed for mouse ECN culture, per media manufacturer's recommendation.

Neuron cultures were fixed on culture day 5 and evaluated for neurite outgrowth with fluorescent immunostaining and nuclear staining as summarized in Figure 2. For these cultures, detection settings were optimized to include cells that met nuclear and soma minimum size criteria that are consistent with characteristics of neurons that were viable at the time of fixation. The Gen5 neurite outgrowth module detection settings used are detailed in Table 1. Detection parameters are flexible and intended to provide users the ability to optimize analysis as desired across a range of expected cell characteristics.

iPSC-derived neuron culture response to outgrowth stimulation and inhibition

Neuron culture outgrowth in response to treatment was first evaluated for iPSC-derived cultures. Results of the Gen5 neurite outgrowth module analysis are automatically reported for both image-level metrics (e.g., total outgrowth

length in the image), as well as cell-level average values (e.g., per-cell average neurite length). Analysis was performed independently for each antibody, and outgrowth dose–response curves for β -tubulin evaluation (Figure 4C) and MAP2 staining evaluation (Figure 4D) are presented for several outgrowth parameters.

For iPSC-derived neurons, responses for each drug were consistent with previous reports of the ability of the drugs to enhance (staurosporine and blebbistatin) or reduce (6BIO and triptolide) neurite outgrowth.⁹ However, blebbistatin produced a relatively small (approximately 20%) increase in total outgrowth for iCell GlutaNeurons, compared to staurosporine. Staurosporine promoted neurite outgrowth until the highest concentrations tested, where significant cell death was abruptly observed, consistent with previous reports.⁹ To estimate the drug effect through fitting, the highest drug concentration for staurosporine was omitted from the four-parameter fit.

As opposed to the two stimulatory drugs tested, both 6BIO and triptolide demonstrated substantial reductions in neurite outgrowth with typical four-parameter dose–response relationships. In addition to reductions in total outgrowth measured at the image-level, the average per-cell neurite length, branch count, and neurite number were all reduced with application of both 6BIO and triptolide (Figure 4C).

The results obtained with β -tubulin and MAP2 staining evaluations (compare Figure 4C and D) largely indicated general agreement on neurite outgrowth properties with some exceptions. For triptolide, both staining evaluations provided similar outgrowth inhibition and dose–response characteristics. For 6BIO, however, β -tubulin staining indicated a greater degree of inhibition compared to MAP2. It is possible that this difference indicates that 6BIO has a greater inhibitory effect on putative axonal outgrowth compared to dendritic outgrowth.

When cell count values are consistent, total image level outgrowth reflects the average outgrowth of any individual cell. However, if cell numbers are changing, such as with loss of neuron viability, it is often informative to also evaluate the per-cell outgrowth average. In addition to image-level results for total outgrowth, the Gen5 neurite outgrowth module calculates the per-cell average neurite outgrowth values using the soma count. For these inhibitory treatments, both the per-cell average and image average outgrowth were in general agreement, indicating the effect on outgrowth occurred at the per-cell level and not only at the image level. This is consistent with the specific inhibitory effect of 6BIO and triptolide on neurite outgrowth and not simply a reflection of a general loss of cell viability.

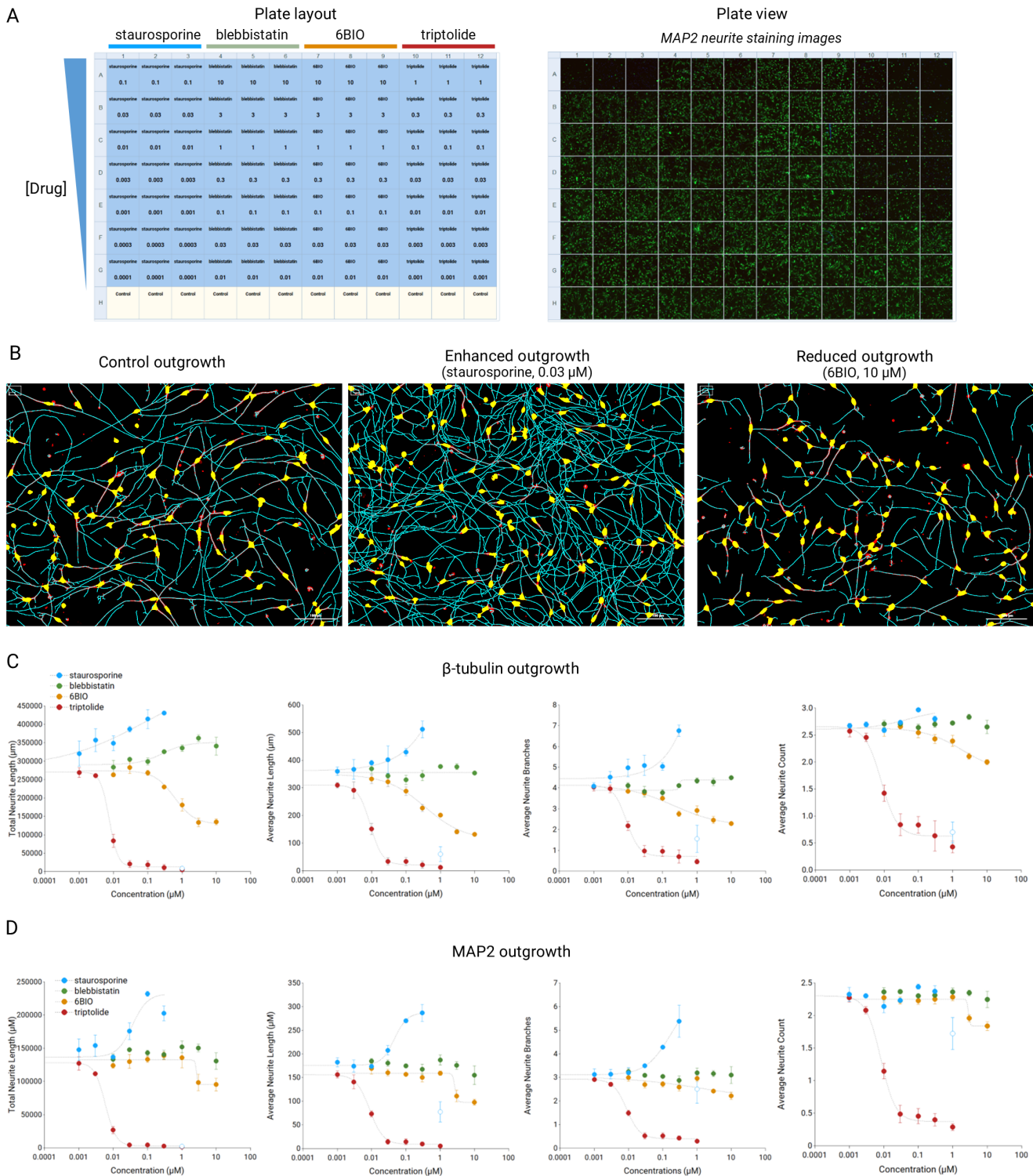


Figure 4. iPSC-derived neuron response to outgrowth enhancers and inhibitors. (A) Plate layout indicating dose–response curves for four drugs tested in outgrowth assay. Plate view shows single image from montage of MAP2 immunofluorescence staining across the plate. (B) Automated image analysis overlay display of the detected soma (yellow) and neurite skeletons (cyan) for three different example images of β -tubulin staining. Scale bars correspond to 100 μm . (C) Dose–response curves for each treatment are plotted for four outgrowth metrics evaluated by β -tubulin staining. Plots depict technical replicate mean ($N = 3$) and standard deviation for each condition. Four-parameter fit lines (dashed black lines) are shown for each curve as indicated. Staurosporine treatment at the single highest concentration is omitted from fitting (open blue circle) to estimate drug response. (D) Dose–response curves for each treatment are plotted for four outgrowth metrics evaluated by MAP2 staining. Plots depict technical replicate mean ($N = 3$) and standard deviation for each condition. Four-parameter fit lines (dashed black lines) are shown for each curve as indicated. Staurosporine treatment at the single highest concentration is omitted from fitting (open blue circle) to estimate drug response.

Cryopreserved mouse cortical culture outgrowth response evaluation

Parallel investigation of outgrowth was undertaken for cryopreserved primary mouse cortical cultures, and was evaluated over the same time course, drug concentration series, and immunohistochemistry approach. Figure 5A shows example images of neurite outgrowth evaluated in control wells and wells treated with positive and negative effectors as indicated after five days of culture. To simplify comparison against iPSC-derived cultures, neurite outgrowth results are presented only for β -tubulin staining.

Blebbistatin produced a large increase in neurite outgrowth in mouse cortical cultures, demonstrated by dose–response evaluations across multiple parameters using both Gen5 neurite outgrowth module analysis (Figure 5B) and cell-averaged analysis (Figure 5C). Interestingly, blebbistatin was the only drug that demonstrated a dose-dependent increase in the number of somas (Figure 5B). As blebbistatin inhibits myosin II implicated in both apoptosis and neuronal outgrowth¹⁹, it is possible that blebbistatin is protective against some of the apoptotic cell loss related to primary cell culture cryopreservation.

Staurosporine, however, demonstrated a complex effect in primary mouse neurons that differed from the relatively robust and consistent outgrowth enhancement observed for iPSC-derived neurons. Cell viability was reduced, as soma counts, total outgrowth, and total branches all decreased with increasing concentrations (Figure 5B). However, the cells that did survive at higher staurosporine concentrations exhibited a greater average number of outgrowths and branches, concurrent with a shorter measured average length (Figure 5C). This combination of effects suggests staurosporine may promote neurite protrusion in this model, but not overall length.

Although iPSC-derived neuron outgrowth was notably inhibited by triptolide, outgrowth of mouse ECN-cultured neurons was much less sensitive to triptolide as reflected in the reduced effect size and comparatively shifted dose–response curve across multiple measures of outgrowth (Table 2). Although triptolide resulted in a relatively small decrease in total neurite length at the highest concentrations tested (Figure 5B), the average length and branching count of the surviving cells was unchanged (Figure 5C); the absence of average per-cell effects suggests a general decrease in neuron viability that was consistent with the observed decrease in soma counts (Figure 5B).

Comparative summary of iPSC-derived and primary mouse neuron outgrowth

Table 2 provides a summary of the Gen5 software neurite outgrowth module measurements for both iPSC-derived and mouse neuron culture models. Control well averages are indicated for each culture type, as well as percent effect size (relative to control well values) and IC/EC₅₀ values across outgrowth metrics. For most treatments, outgrowth metric responses were adequately fit with four-parameter dose–response relationships and IC/EC₅₀ values automatically calculated in the Gen5 software for imaging and microscopy. In some cases, however, plateaus for concentration-dependent effects were not well resolved. In those cases, reported effect size and IC/EC₅₀ values were instead reported at 50% of the maximal response of the highest test concentration using fit interpolation values in the Gen5 software.

For each metric, Z-scores were calculated in Gen5 software to determine whether treatment means were significantly different from the control mean for each outgrowth parameter. Outgrowth parameters with Z-score absolute values greater than two across multiple consecutive concentrations were considered to have a parameter mean that was significantly different from control. Effect size and IC/EC₅₀ values are included for treatments with significant responses in Table 2. Outgrowth parameters that did not result in significant differences from control are indicated with “ns.”

In addition to the default parameters measured by the Gen5 neurite outgrowth module, an additional parameter calculating the percentage of neurons that had outgrowth is included in Table 2. For this percentage evaluation, only cells that exhibited multiple (> 1) neurite counts were considered to have significant outgrowth and included in the percentage. This parameter was generated using the neurite module “Group Neurons” functionality to count cells and create subpopulations based on different available measurements. Neuron grouping criteria are flexible to permit user-specified groupings based on multiple parameters such as soma size, signal intensity, or neurite count.

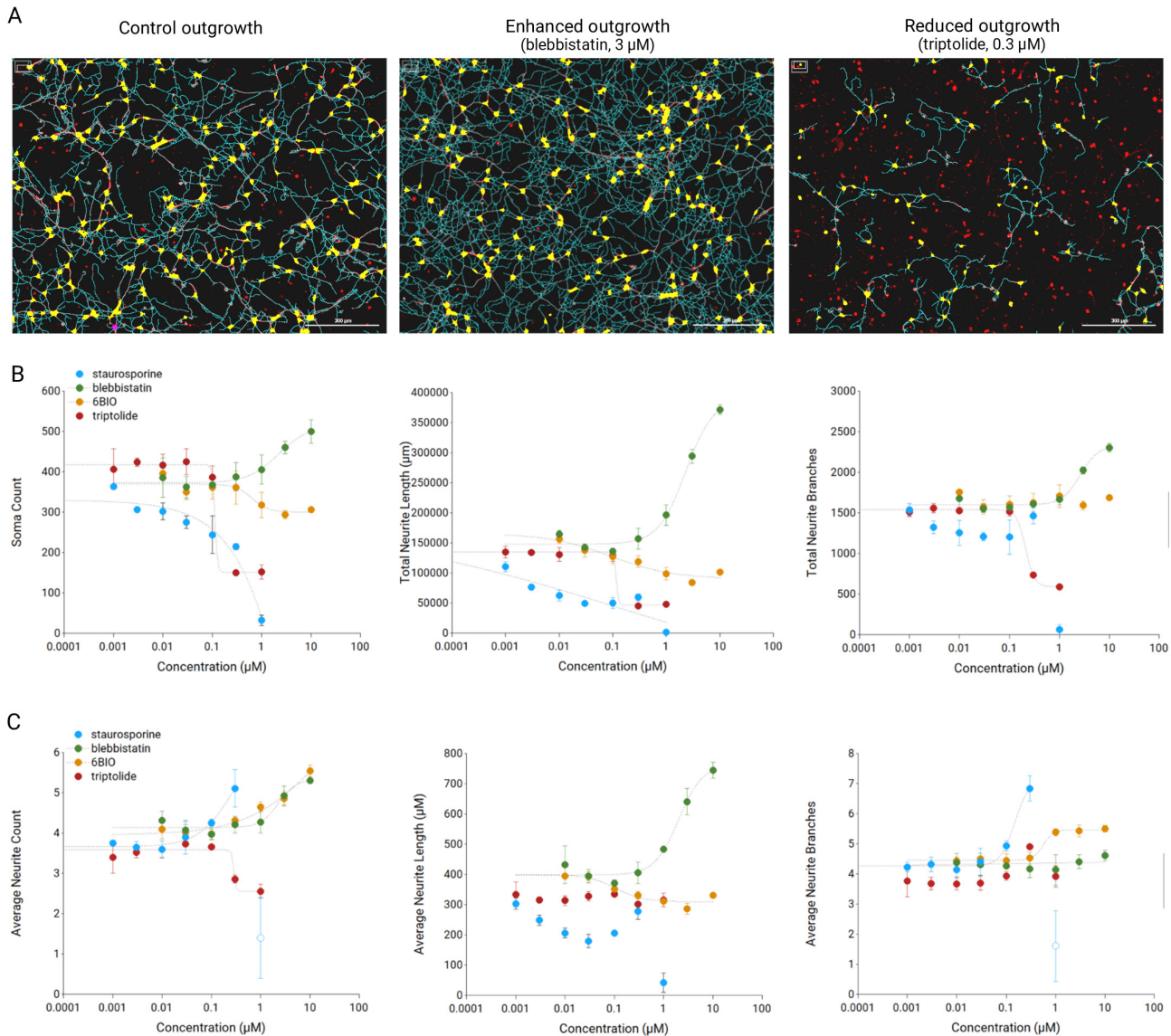


Figure 5. Cryopreserved mouse cortical culture response to effectors of neurite outgrowth. (A) Automated image analysis overlay displays the detected soma (yellow fill) and skeletonized neurites (cyan lines) for three different example images of β -tubulin staining. Scale bar corresponds to 300 μm . (B) Dose–response curves of neurite outgrowth parameters for β -tubulin staining evaluated at the image level, including soma count (left panel), total neurite length (middle panel), and total neurite branches (right panel) for four drugs as indicated. Plots depict technical replicate mean ($N = 3$) and standard deviation for each condition. For data series that conformed to a four-parameter fit, fit lines (dashed lines) are shown for each curve as indicated. (C) Dose–response curves for neurite outgrowth parameters evaluated by per-cell average for neurite count (left panel), average neurite length (middle panel), and average neurite branches (right panel). Plots depict technical replicate mean ($N = 3$) and standard deviation for each condition. For data series that conformed to a four-parameter fit, fit lines (dashed black lines) are shown for each curve as indicated. The highest concentration data point was omitted from staurosporine dose–response curve fitting as indicated (blue open circles) to permit fitting over the remaining concentrations.

Table 2. Neurite outgrowth effect summary for iPSC-derived and primary mouse culture.

Neurite Outgrowth Summary										
	Untreated		Staurosporine		Blebbistatin		6BIO		Triptolide	
	Value (%CV)		Percent maximum relative change EC/IC ₅₀ (μM)							
	iPSC-Derived	Mouse Cortical	iPSC-Derived	Mouse Cortical	iPSC-Derived	Mouse Cortical	iPSC-Derived	Mouse Cortical	iPSC-Derived	Mouse Cortical
Soma Count	814 (11.7)	398 (6.7)	-82% 0.35 μM	-92%* 0.32 μM*	ns	+29% 2.2 μM	ns	-25% 0.64 μM	-68% 0.0077 μM	-62% 0.11 μM
Total Neurite Length	257,000 μm (11.6)	157,000 μm (7.7)	+67%* 0.007 μM*	-62%* 0.001 μM*	+36% 0.26 μM	150% 2.3 μM	-50% 0.61 μM	-42% 0.75 μM	-95% 0.0076 μM	-70% 0.12 μM
Average Neurite Length	317 μm (10.1)	395 μm (8.6)	+61%* 0.1 μM*	Complex	ns	+94% 2.0 μM	-65% 0.4 μM	-22% 0.10 μM	-93% 0.011 μM	ns
Total Neurite Branches	3472 (13.1)	1643 (6.6)	+64%* 0.01 μM*	Complex	ns	+42% 2.6 μM	-33% 2.2 μM	ns	-89% 0.0083 μM	-64% 0.21 μM
Average Neurite Branches	4.3 (7.8)	4.1 (7.5)	+57% 0.1 μM*	+75% 0.15 μM	ns	ns	-50% 0.25 μM	+33% 0.56 μM	-84% 0.011 μM	ns
Total Neurite Area	613,000 μm ² (8.4)	526,000 μm ² (7.1)	+31% 0.029 μM	-75%* 0.004 μM*	ns	+112% 1.9 μM	-45% 0.92 μM	-44% 0.13 μM	-95% 0.0081 μM	-75% 0.15 μM
Neurite Thickness	2.4 μm (4.3)	3.4 μm (2.5)	ns	-31% 0.11 μM	ns	-15% 2.9 μM	+31% 0.27 μM	ns	+29% 0.0069 μM	-19% 0.26 μM
Average Neurite Count	2.5 (4.1)	4.0 (6.5)	+19% 0.046 μM	+28%* 0.12 μM*	ns	+34% 2.3 μM	ns	+39%* 2.0 μM*	-75% 0.0087 μM	-36% 0.29 μM
Soma Size	13.2 μm (1.4)	19.7 μm (0.9)	-10%* 0.44 μM*	-30%* 0.34 μM*	ns	ns	ns	ns	-10% 0.0046 μM	-23% 0.21 μM
Nucleus Size	9.2 μm (1.2)	10.8 μm (1.8)	Complex	ns	ns	ns	+8.7%* 0.14 μM	ns	+6.6% 0.30 μM	ns
Percentage Neurons with Outgrowth	83.1% (3.3)	91.4% (2.6)	-85% 0.87 μM	-76% 0.87 μM	ns	+6% 1.3 μM	-14%* 1.4 μM*	ns	-81% 0.0096 μM	-25% 0.29 μM

*Indicates that the effect size and EC/IC₅₀ were estimated at 50% maximum/minimum response in cases where fit and response did not plateau.

"Complex" indicates that the effect was not monotonic.

Conclusion

Automated solutions for image-based neurite outgrowth are essential to enable rapid and high-throughput neurobiology investigations at scale. The Agilent BioTek Gen5 neurite outgrowth module described here provides a flexible and powerful solution that leverages the advantages of an automated, high-throughput system for multimodal image analysis. A key feature of the Gen5 neurite outgrowth module for neurite outgrowth assays is the flexibility of multichannel analysis across multiple fluorescence channels and modalities to support a broad range of neurite outgrowth approaches.

This study has provided a proof-of-principle demonstration for neurite outgrowth analysis of both iPSC-derived and primary mouse neuron culture models relevant to a broad range of neurobiology research areas. We have focused on evaluating these key neurite outgrowth models in a commonly used immunohistochemistry-based approach to demonstrate the usability and performance of the platform. Agilent BioTek Gen5 microplate reader and imager software integrated the automated image capture, processing, and neurite outgrowth detection within a single interface and in a streamlined step-wise process. Data plotting and fitting capabilities of the Gen5 microplate reader and imager software readily transformed the neurite image detection results into quantitative analysis of the treatment effects. In both culture models tested, significant dose-response effects were measured across multiple parameters of neurite outgrowth for several modulators of neuronal outgrowth.

References

1. Radio, N.M.; Mundy, W.R. Developmental Neurotoxicity Testing in Vitro: Models for Assessing Chemical Effects on Neurite Outgrowth. *NeuroToxicology* **2008**, *29*, 361-376. <https://doi.org/10.1016/j.neuro.2008.02.011>
2. Blum, J; Masjosthusmann, S.; Bartmann, K.; Bendt, F.; Dolde, X.; Dönmez, A.; Förster, N.; Holzer, A-K.; Hübenal, U.; Keßel, H.E.; et. al. Establishment of a Human Cell-Based in Vitro Battery to Assess Developmental Neurotoxicity Hazard of Chemicals. *Chemosphere* **2023**, *311*, 137035. <https://doi.org/10.1016/j.chemosphere.2022.137035>
3. Al-Ali, H.; Beckerman, S.; Bixby, J.L., Lemmon, V.P. In Vitro Models of Axon Regeneration. *Exp Neurol* **2017**, *287*, 423-434. <https://doi.org/10.1016/j.expneurol.2016.01.020>
4. Logan, S.; Arzua, T.; Canfield, S.G.; Seminary, E.R.; Silson, S.L.; Ebert, A.D.; Bai, X. Studying Human Neurological Disorders Using Induced Pluripotent Stem Cells: From 2D Monolayer to 3D Organoid and Blood Brain Barrier Models. *Compr Physiol* **2019**, *9*, 565-611. <https://doi.org/10.1002/cphy.c180025>
5. Farkhondeh, A.; Li, R.; Gorshkov, K.; Chen, K.G.; Might, M.; Rodems, S.; Lo, D.C.; Zheng, W. Induced Pluripotent Stem Cells for Neural Drug Discovery. *Drug Discovery Today* **2019**, *24*, 992-999. <https://doi.org/10.1016/j.drudis.2019.01.007>
6. Radio, N.M; Breier, J.M.; Shafer, T.J.; Mundy, W.R. Assessment of Chemical Effects on Neurite Outgrowth in PC12 Cells Using High-Content Screening. *Toxicological Sciences* **2008**, 106-118. <https://doi.org/10.1093/toxsci/kfn114>
7. Dravid, A.; Svirskis, D.; O'Carroll, S.J. Optimised Techniques for High-Throughput Screening of Differentiated SH-SY5Y Cells and Application for Neurite Outgrowth Assays. *Sci Reports*, **2021**, *11*, 23935. <https://doi.org/10.1038/s41598-021-03442-1>
8. Blackmore, M.G.; Moore, D.L.; Smith, R.P.; Goldberg, J.L.; Bixby, J.L.; Lemmon, V.P. High-Content Screening of Cortical Neurons Identifies Novel Regulators of Axon Growth. *Mol and Cellular Neurosci* **2010**, *44*, 43-54. <https://doi.org/10.1016/j.mcn.2010.02.002>
9. Sherman, S.P.; Bang, A.G. High-Throughput Screen for Compounds that Modulate Neurite Growth of Human Induced Pluripotent Stem Cell-Derived Neurons. *Dis Model Mech* **2018**, *11*, dmm031906. <https://doi.org/10.1242/dmm.031906>
10. Wang, Y.; Xu, Y.; Liu, Q.; Zhang, Y.; Gao, Z.; Yin, M.; Jiang, N.; Cao, G.; Yu, B.; Cao, Z.; et. al. IIA-Related Actomyosin Contractility Mediates Oxidative Stress-Induced Neuronal Apoptosis. *Front Mol Neurosci* **2017**, *10*, 75. <https://doi.org/10.3389/fnmol.2017.00075>

www.agilent.com/lifesciences/biotek

For Research Use Only. Not for use in diagnostics procedures.

RA45404.3322222222

This information is subject to change without notice.

© Agilent Technologies, Inc. 2024
Published in the USA, May 15, 2024
5994-7380EN

